Volume 9, Issue 6, June – 2024 International Journal of Innovative Science and Research Technology
ISSN No:-2456-2165 https://doi.org/10.38124/ijisrt/IJISRT24JUN167

Elemental Composition and Surface Properties of Agro-Wastes of Doum Palm, African Elemi, and Desert Date Seed Shells Obtained from Jos Town, Plateau State, Nigeria

[1]Moses Stephen Anyebe
[1]Department of Industrial Chemistry/Petrochemical Technology, School of Science Laboratory Technology, University of Port Harcourt, Choba, River State, Nigeria

*[2]Pereware Adowei
*[2]Department of Pure and Industrial Chemistry, Faculty of Science,University of Port Harcourt, Choba, River State, Nigeria

Corresponding Author:- *[2]Pereware Adowei

Abstract:- Improvement in agriculture has significantly enhanced living standards of the people, however, agriculture has also caused negative impacts on environmental health as a consequence of agro-waste generation. Therefore, the objective of this paper was to investigate the elemental composition and surface properties of agro-wastes of Doum palm (DPS), African elemi (AES), and Desert Date (DDS) seed shells sourced from open markets in Jos Town, Plateau State, Nigeria using various appropriate standard methods. The BET surface area, BJH adsorption cumulative pore volume, and pore sizes were 418 m^2/g, 0.21 cm^3/g, and 2.10nm for DDS; 471 m^2/g, 0.26 cm^3/g, and 2.13nm for AES and 285 m^2/g, 0.17 cm^3/g, and 2.14nm for DPS respectively. The data obtained confirms the micro-porous nature of these agricultural seed shell wastes. X-ray Fluorescence (XRF) study shows variances in elemental composition, notably in SiO_2, CaO, Al_2O_3, K_2O, and Cl content. The surface morphology characterization reveals the presence of hydroxyl (-OH) and carbonyl (C=O) functional groups, indicating possible adsorption sites. DPS, AES, and DDS have particular BJH pore sizes and BET surface areas, exhibiting Type I microporous properties. The elemental composition and surface characteristics show promising properties for their use as adsorbents for CO_2 capture, organic and inorganic contaminants removal and COD reduction in wastewater. However, the variances observed highlights the necessity to adapt activation procedures before utilizing them for adsorption studies.

Keywords:- *CO_2 Capture, Adsorption, Doum Palm, African Elemi Desert Date; Adsorption.*

I. INTRODUCTION

Agro-waste is defined as waste left over after cultivating and processing agricultural products like fruits, vegetables, dairy and grains, as well as meat, poultry and crops. Generally agricultural wastes are classified into four types: crop waste (rice husk, wheat straws, sugarcane bagasse), animal waste (animal excreta, dead animals), processing waste (packaging material, fertilizer cans) and hazardous waste (pesticides, insecticides). A yearly production of agricultural waste of roughly 998 million tonnes is estimated. In comparison to total solid waste generated on farms, approximately 80% of it is organic waste. Most farmers dump this waste in pits, allowing the majority of the area free for farming. Also, much of the agricultural waste is used as fodder for animals. Instead of dumping, the agricultural waste can be utilized to make other valuable products, like animal manures used for making fertilizer, as it contains 19%, 38% and 61% of nitrogen, phosphorous and potassium, respectively. They have good implications for agricultural growth and productivity. A second, use of agriculture waste is for synthesis of gas for heating and cooking purposes (Bilal et al., 2023; Wang et al., 201; Abdelfattah et al. 2016; Adowei, 2024). Agriculture wastes have recently emerged as a low-cost alternative for the adsorption-based effluent treatment of wastewater contaminated with heavy metals (Akande and Olorunnisola, 2018). Low-cost agricultural waste includes coconut husk, sawdust, sugarcane bagasse, neem bark and rice husk. The environment friendly and sustainable heterogeneous catalysts that contribute in the cost-effective synthesis of biodiesel are made from rice husk (Yang yang et al., 2016). In addition to rice husk, other agricultural waste products with substantial amounts of silica that can be recovered include sugarcane bagasse and bamboo leaf (Yang yang et al., 2016). Agricultural waste material has also been utilized for sustainable construction material to develop waste-create bricks (Zaket al., 2021). Moreso, agricultural waste materials have been converted into carbon nanostructures which can be possibly used for various purposes (Wang and Chu, 2013; Merret *et al.,* 2002)

Agricultural waste materials, especially those containing cellulose, have the ability to absorb a variety of contaminants. Hemicellulose, lipids, lignin, proteins, starch, hydrocarbons, water and simple sugars are the main components of agricultural waste products, and they contain a range of functional groups. Agricultural waste products are

ISSN No:-2456-2165 https://doi.org/10.38124/ijisrt/IJISRT24JUN167

a feasible choice for water and wastewater remediation due to their unique abundant availability, chemical composition, low cost and renewable nature. Since agricultural waste have a low ash content and a moderate hardness, it is a promising source for production of activated carbon. As a result, converting agricultural leftovers into low-cost adsorbent materials is a viable technique for addressing environmental issues while lowering preparation expenses (Zaket al., 2021

A lot of research is being carried out to covert agro-industrial waste into low cost adsorbents, which include stones and shells of fruits like almonds, peanuts husks, olive wastes, cherries, apricots stones as well as the residue originating from cereals production such as corn, maize, rice and sugarcane bagasse (Ikram et al., 2016).

The Agricultural waste characterization could lead to its non-wasteful utilizations. Surface properties have an enormous effect on the success or failure of a biomaterial device, thus signifying the considerable importance of and the need for adequate characterization of the biomaterial surface (Merret *et al.,* 2002). Buddy (2013) investigated the surface properties and surface characterization of biomaterials showing that atoms and molecules that reside at surfaces have a special organization and reactivity, and require special methods to characterize them and novel methods to tailor them. They drive many of the biological reactions that occur in response to the biomaterial (protein adsorption, cell adhesion, cell growth, blood compatibility, etc.).

No single technique can provide all the information, and quite often, different analytical tools are required to address a problem related to biomaterials research. To obtain surface chemical and morphological information, spectroscopic techniques such as X-ray photoelectron spectroscopy (XPS), Auger electron spectroscopy (AES), secondary ion mass spectroscopy (SIMS), and microscopic methods such as confocal microscopy, scanning electron microscopy, atomic force microscopy (AFM) are typically carried out. Other surface characterization methods such as contact angle (CA) measurement and ellipsometry are also widely used in biomaterials research. It should be emphasized that each technique has its strengths and weaknesses, and complete characterization frequently requires more than one method. Carbon dioxide capture is also an important component of environmental sustainability (Erans et al., 2022, Kainth et al., 2024)

Hence, the objective of this paper was to investigate the elemental composition and surface properties of agro-wastes of Doum palm (DPS*),* African elemi (AES), and Desert Date (DDS) seed shell sourced from open markets in Jos Town, Plateau State, Nigeria with the aim of utilizing them in adsorption studies for CO_2 capture.

II. MATERIALS AND METHODS

➢ *Study Area and Sample Collection*

The seeds of Doum palm (*Hyphaene thebaica),* African elemi (*Canarium schweinfurthii*), and desert date (*Balanites aegyptiaca*) were procured from the open markets in Jos town, Nigeria (Figure 1), owing to their widespread availability in the region.

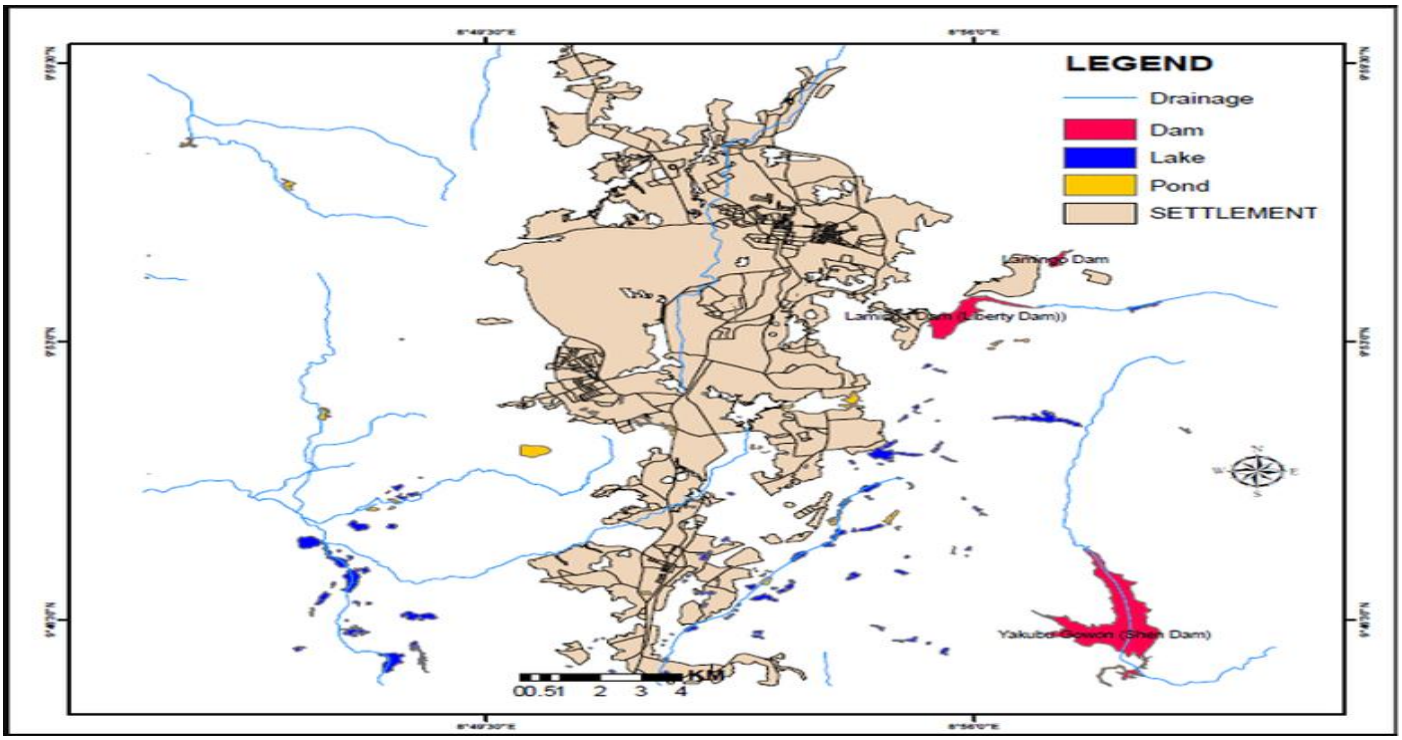

Fig 1 Map of Jos Metropolis Plateau State, Nigeria
Source: National Centre for Remote Sensing, Jos As Published By Ali *Et Al.,* 2016

ISSN No:-2456-2165 https://doi.org/10.38124/ijisrt/IJISRT24JUN167

- *Sample Preparation:*

Following collection, the samples underwent a cleaning process with distilled water to eliminate dirt and dust particles. Subsequently, the seeds were sun-dried to eliminate moisture. The dried seed shells were then finely ground using a high-power grinding machine and further subjected to 24 hours of oven- drying at 110 °C to ensure complete moisture removal. These processed samples were stored in a desiccator and remained in use throughout the experiment. The raw and powder samples of Doum palm shells (DPS), the African elemi shells (AES) and the desert date shells (DDS) are presented in Figure 2.

Fig 2 Showing the Raw and Powder Samples of Doum Palm Shells (DPS), the African Elemi Shells (AES) and the Desert Date Shells (DDS)

- *Determination of Specific Gravity*

ASTM C 127-07 (2007), a standard that is used to determine the specific gravity of materials, was employed to ascertain specific gravities of of Doum palm shells (DPS), the African elemi shells (**AES)** and the desert date shells (DDS). Specific gravity given with Equation (1),

$$SG = \frac{W_2 - W_1}{(W_4 - W_1) - (W_3 - W_2)} \quad (1)$$

Where, SG=Specific gravity; W1=Weight of empty density bottle (g); W2=Weight of density bottle +Sample (g); W3=Weight of density bottle + Sample +Water (g); W4=Weight of density bottle + Water (g).

- *Determination of Moisture Content (MC)*:

The percentage moisture content (PMC) determined by weighing 1.5g of sample put in a crucible of known mass and placed in an oven set at 105°C ± 5°C for 1 hour. The crucible and its content were removed from the oven allowed to cool to room temperature and reweighed. This process was repeated until the weight after cooling became constant and this was recorded as the final weight. The sample's moisture content was determined using equation (2).

$$\%\, MC = \frac{W_1 - W_2}{W_2} * 100 \quad (2)$$

Where, W1 is the initial weight of briquette sample and W2 is the final weight of briquette sample

- *Determination of Volatile Matter (VM)*:

The percentage volatile matter (PVM) was determined by placing 1.5g of sample in a crucible and kept in a furnace for 8 minutes, at temperature of 550o C ± 5°C and weighted after cooling. The percentage volatile matter of the sample was determined using equation (3)

$$\%\, VM = \frac{W_2 - W_3}{W_3} * 100 \quad (3)$$

Where, W2 is the weight of the oven-dried sample (g); W3 is the weight of the sample after 8 min in the furnace at 550 °C (g)

- *Determination of Ash Content (AC)*:

1.5g of samples are kept in a closed furnace and burnt completely. The weight of the residue was taken with an electronic balance. The percentage weight of residue gives the ash contained in the sample and its determined using equation (4).

$$\%\, AC = \frac{W_4}{W_2} * 100 \quad (4)$$

ISSN No:-2456-2165 https://doi.org/10.38124/ijisrt/IJISRT24JUN167

- *Determination of Fixed Carbon*:

The percentage fixed carbon (FC) was computed by subtracting the sum of VM and AC from 100 as shown in the Equation 5:

$$\% FC = 100 - [MC + VM + AC] \quad (5)$$

- *Ultimate Analysis of Biomass for* Elemental Composition*:*

In accordance to the standard ASTM methods [ASTM D3176-09, ASTM International (2009); ASTM D5373-08 (2008)] for ultimate analysis, the presence of common elements such as C, H, N, and S in biomass and biochar samples was determined through a PerkinElmer Elementar CHNS analyzer. O (wt.%) was measured by the difference of C, H, N, S, and ash from 100. Major inorganic elements in biomass, ash, and biochar samples were resolved using the di-acid digestion method (HNO3 and H2O2, 5:1 v/v) for multi-elemental analysis through a PerkinElmer NexION 300D ICP-MS (inductively coupled plasma-mass spectrometry). The carbon, hydrogen, nitrogen, and Sulphur contents are subtracted from 100 to get the oxygen composition based on these results.

- *Surface Area, Pore Volume, and Pore Size Analysis:*

The surface properties of the samples were determined by the Brunauer–Emmett–Teller (BET) analysis. The pore volume and size were determined by the BJH (Barrett-Joyner-Halenda) analysis, the Dubinin-Astakhov (DA), and the density functional theory (DFT) methods (Aimikhe et al., 2022; Wahby et al 2011)

- *BET Analysis:*

The BET analysis reveals the precise surface area, pore volume, and diameter of the sample. Single-point BET uses one isotherm point for surface area determination, while multipoint BET uses at least three. For this study, 0.3 g of the sample was placed in a BET glass tube and weighed before and after loading. The sample was degassed at 473 K for three hours using a Micromeritics Flow Prep 067 with nitrogen gas to remove bound water. After degassing, the sample was reweighed and analyzed in a Micromeritics TriStar 3000 V4.02 at liquid nitrogen temperature. The device automatically estimated the BET surface area and pore volume/size using a N2 isotherm. The adsorption isotherm equation of Brunauer, Emmett, and Teller (BET) is applied to the data (Aimikhe et al., 2022 Shoaib et al., 2020)

- *Surface Chemistry Assessment:*

Fourier Transform Infrared Spectroscopy (FTIR) identifies chemical bonds and functional groups in activated carbon. This technique helps pinpoint specific functional groups responsible for gas adsorption. The study used a Buck Scientific M530 USA FTIR instrument with a potassium bromide beam splitter and a deuterated triglycine sulfate detector. Spectra were collected and adjusted with Gramme A1 software. A 0.5 mL volume of nujol was mixed with 1.0 g of the AC sample and placed on a salt pellet. FTIR spectra were measured from 4,000 to 600 cm^{-1}, with each spectrum collected over 32 scans at a 4 cm^{-1} resolution. The spectra were combined using summation, and transmitter values were provided.

- *SEM Analysis:*

A Scanning Electron Microscope (SEM) (JEOL, JSM-T330) and an Energy Dispersive X-ray Spectrometer (EDS) were used in combination to analyze the surface morphology of the AC samples and determine their elemental composition. A transmission electron microscope (TEM; JEOL, 2010 UHR) was used to investigate the samples and reveal the porous nature of the adsorbents. The material was applied to the grid using a solvent made up of 40% alcohol for TEM examination (Aimikhe et al., 2022).

III. RESULTS AND DISCUSSION

Proximate Analysis of Raw materials of Doum palm shells (DPS), the African elemi shells (AES) and the desert date shells (DDS): Table 1 presents proximate analysis results for Doum palm shells (DPS), African elemi shells (AES), and desert date shells (DDS). The samples contained 5.09%, 6.06%, and 3.06% moisture; 52.05%, 60.00%, and 55.00% volatile matter; 5.09%, 6.06%, and 3.06% ash; and 32.26%, 28.4%, and 36.4% fixed carbon, respectively. These results indicate high carbon, low ash, and high volatile matter contents, making them suitable for adsorption applications.

Materials with low ash and high carbon content are effective adsorbents. Carbonaceous materials, with their large surface area, can bind strongly to various substances through adsorption and introduce fewer contaminants due to low ash content. Higher volatile matter may increase adsorption capacity by releasing gases during the process. Kumar and Jena, 2015. support these findings, indicating these shells are ideal for removing contaminants from liquids or gases.

Specific gravities of DPS, AES, and DDS are also shown in Table 1. DDS, with a low density of 35.71 g/cm³, has high adsorption potential. However, adsorption efficiency depends on factors like pore structure, surface area, adsorption capacity, mechanical strength, and overall performance. Density must be balanced with surface area, mechanical stability, and porosity for effective adsorption Kumar and Jena, 2015.

Table 1 Specific Gravity and Proximate Analysis of DPS, AES and DDS

S/NO	Sample	SG (gcm^{-3})	AC (%)	VM (%)	MC (%)	FC (%)
1.	DPS	39.29	10.6 ±0.002	52.05 ±0.01	5.09 ±0.002	32.26
2.	AES	63.93	11.54 ±0.005	60 ±0.002	6.06 ±0.001	28.4
3.	DDS	35.71	8.54 ±0.005	55 ±0.002	3.06 ±0.001	36.4

SG = Specific Gravity; AC = Ash Content; VC = Volatile Matter; MC = Moisture Content and FC = Fixed Carbon

ISSN No:-2456-2165 https://doi.org/10.38124/ijisrt/IJISRT24JUN167

➢ *Surface Area Analysis of Raw Materials of Doum Palm Shells (DPS), the African Elemi Shells (AES) and the Desert Date Shells (DDS):*

Surface area analysis refers to the measurement of a particle's available surface. It is important because it is the means by which a solid interacts with its surroundings, whether they are gases, liquid, or other solids. Surface analysis measurements provide a means to correlate performance with surface composition and structure. This knowledge can be used to accelerate the development of new materials or improve existing materials' performance. The results of the various Surface Area Analysis of raw materials of Doum palm shells (DPS), the African elemi shells (AES) and the desert date shells (DDS) are presented in Figure 5-7 shows N2 adsorption–desorption isotherms at 77 K for DPS, AES, and DDS samples, indicating they are microporous solids with type I isotherms.

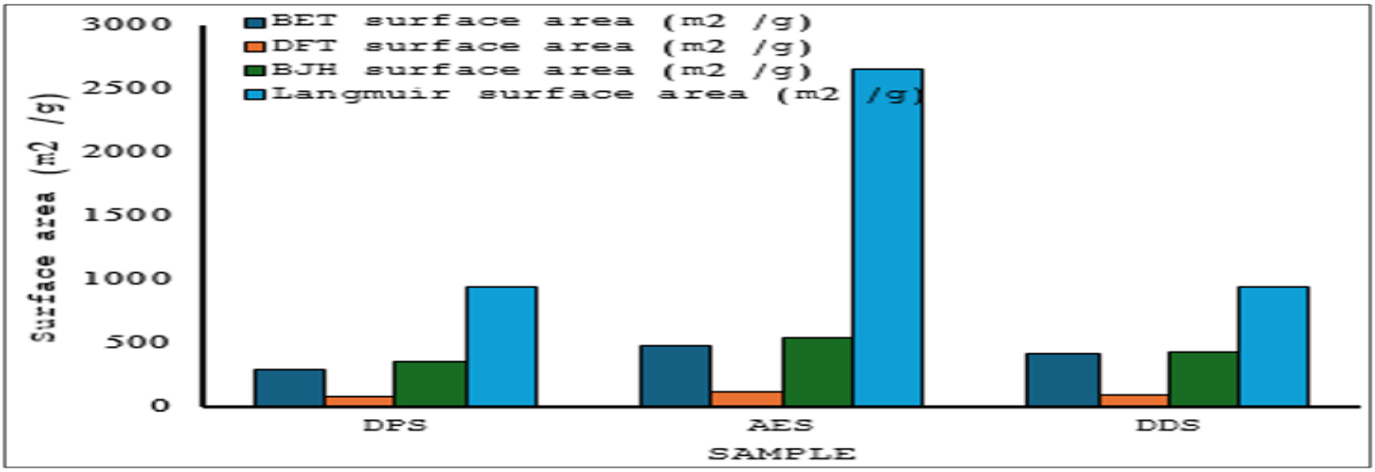

Fig 3 Surface Area of DPS, AES and DDS Sample

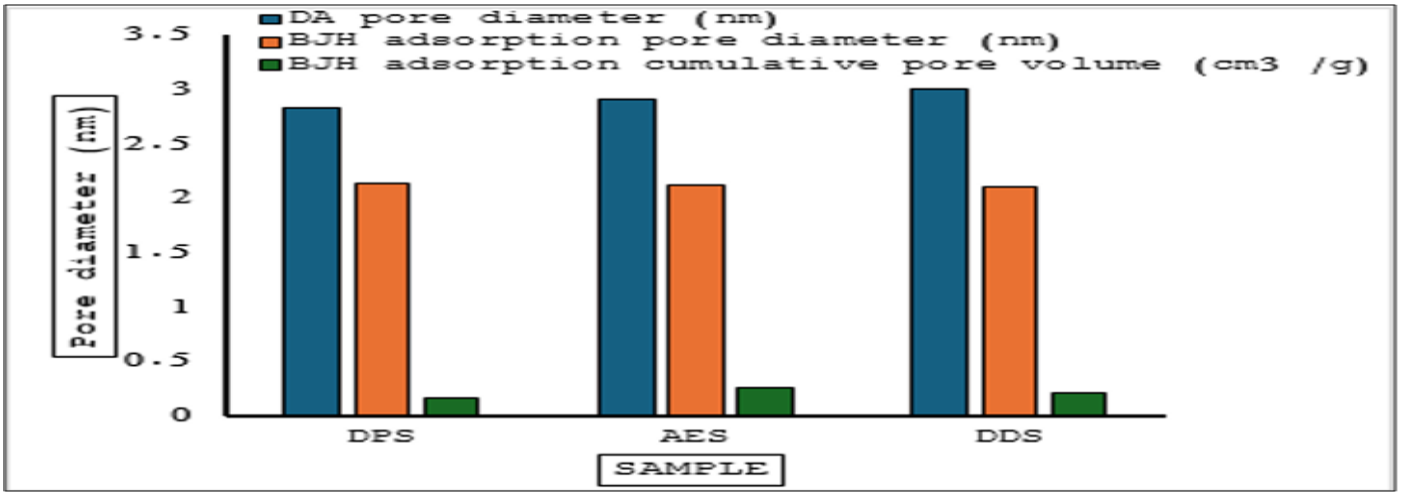

Fig 4 Pore Diameter of DPS, AES and DDS Samples

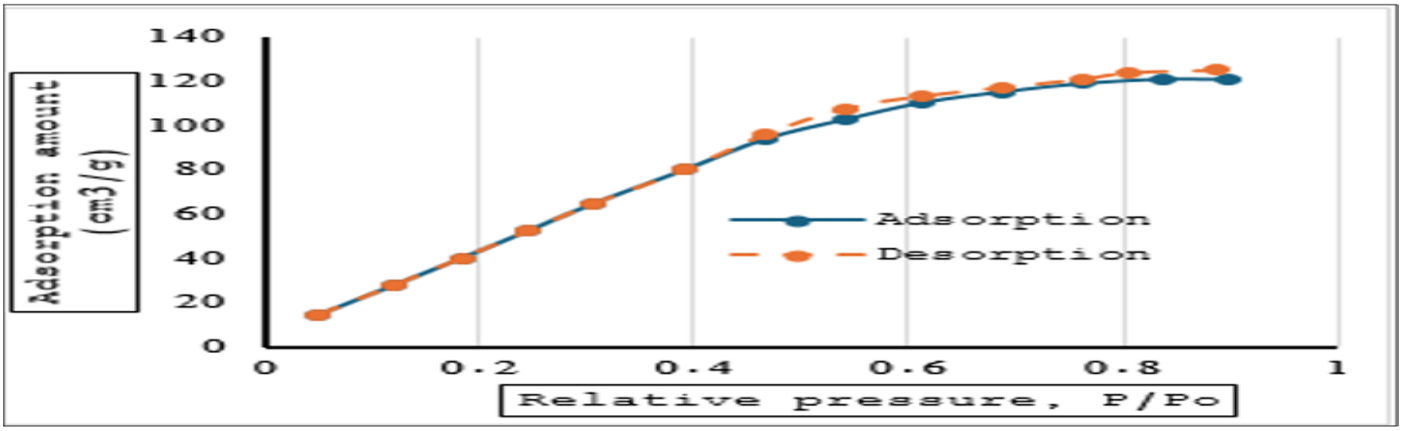

Fig 5 N_2 Adsorption–Desorption Isotherms for DPS Sample

ISSN No:-2456-2165 https://doi.org/10.38124/ijisrt/IJISRT24JUN167

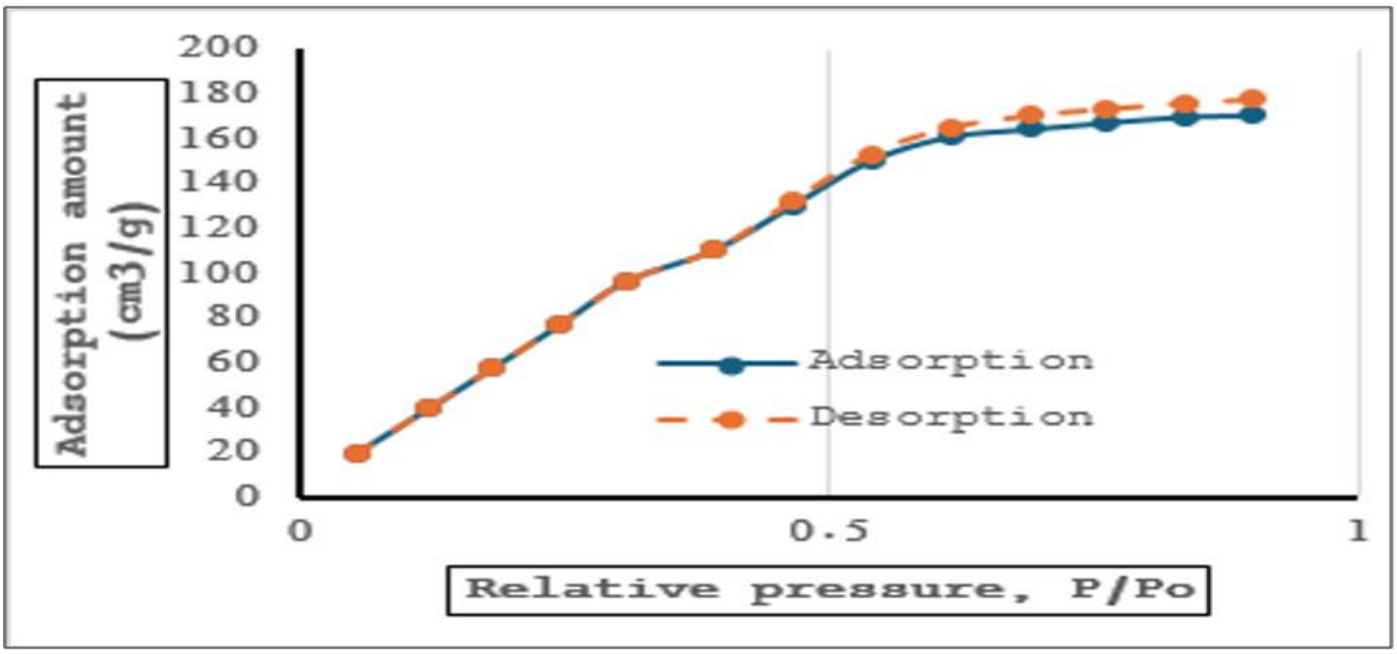

Fig 6 N_2 Adsorption–Desorption Isotherms for AES Sample

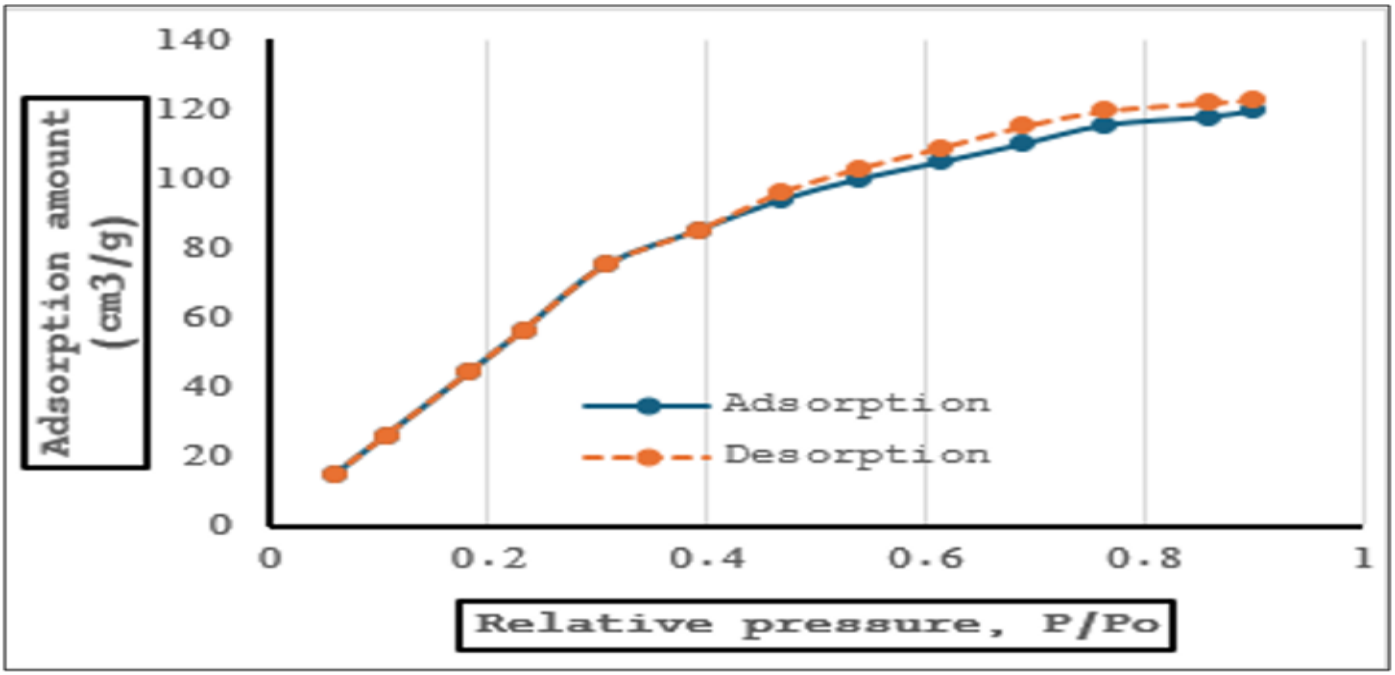

Fig 7 N_2 Adsorption–Desorption Isotherms for DDS Sample

The Dubinin-Astakhov (DA) pore size distribution is shown in Figure 8-10. AES has the largest surface area (471 m^2/g), followed by DDS (418 m^2/g), and DPS (285 m^2/g), as seen in Figure 3. These results align with Langmuir, BJH, and DFT evaluations. Figure 4 shows AES has the highest cumulative pore volume, indicating greater porosity, while DPS has the lowest. AES and DDS have average pore diameters over 2 nm, suggesting narrow mesopores, whereas DPS, with pore sizes under 2 nm, is classified as microporous.

The microporous nature of DPS, AES, and DDS allows efficient pollutant adsorption, with BJH pore sizes of 2.14 nm, 2.13 nm, and 2.10 nm, respectively. The Langmuir model best describes their adsorption mechanism, primarily involving monolayer adsorption. BET and DFT surface areas confirm their potential as effective adsorbents: DPS (285 m^2/g BET, 77 m^2/g DFT), AES (471 m^2/g BET, 114 m^2/g DFT), and DDS (418 m^2/g BET, 87 m^2/g DFT). However, maximal CO_2 adsorption isn't solely determined by surface area or pore volume. Modifying these seed shells could enhance their adsorption capacity further.

ISSN No:-2456-2165 https://doi.org/10.38124/ijisrt/IJISRT24JUN167

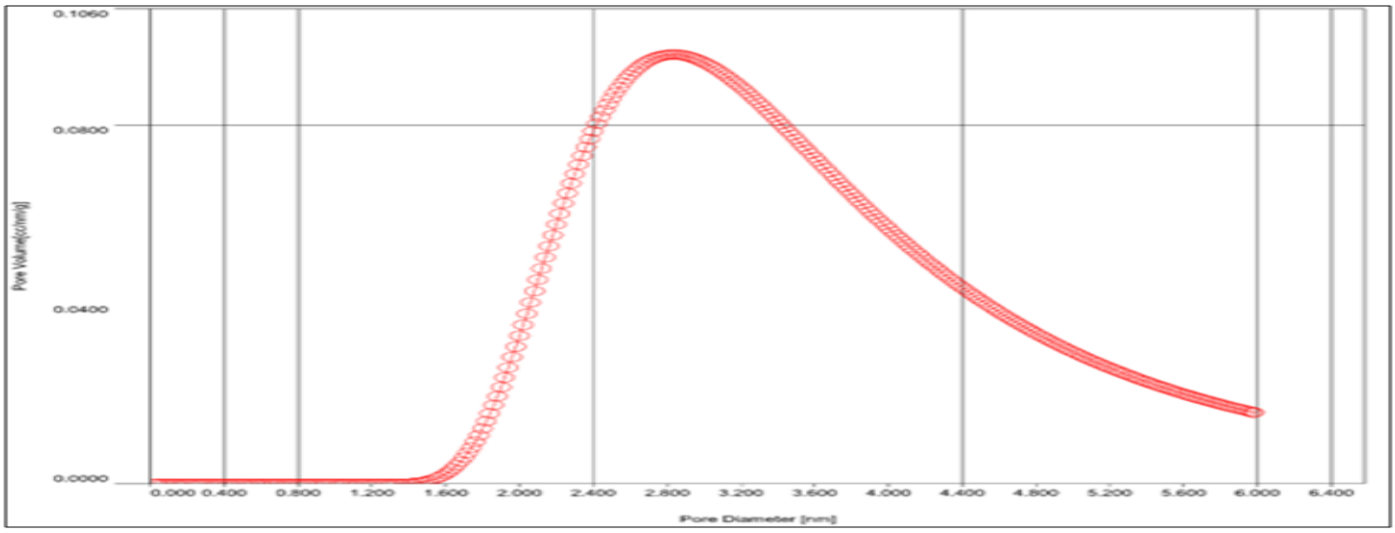

Fig 8 Dubinin-Astakhov (DA) Modal Pore Size Distribution for DPS Sample
Showing a Monolayer Adsorption Pore Diameter of 2.92nm

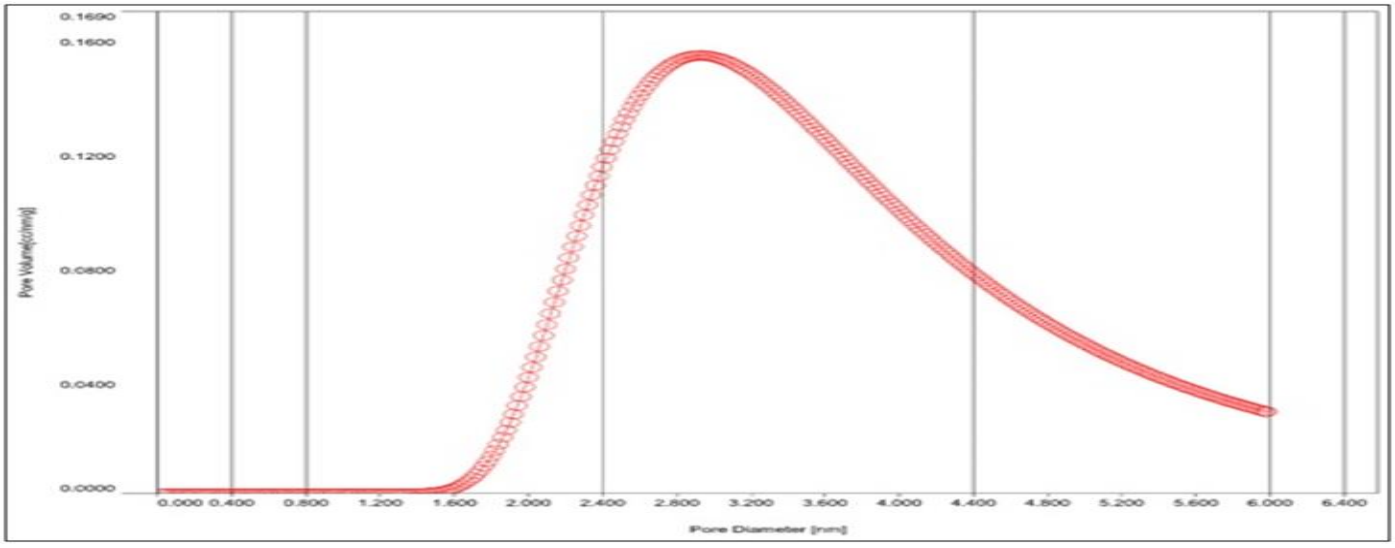

Fig 9 Dubinin-Astakhov (DA) Modal Pore Size Distribution for AES Sample
Showing a Monolayer Adsorption Pore Diameter of 2.92nm

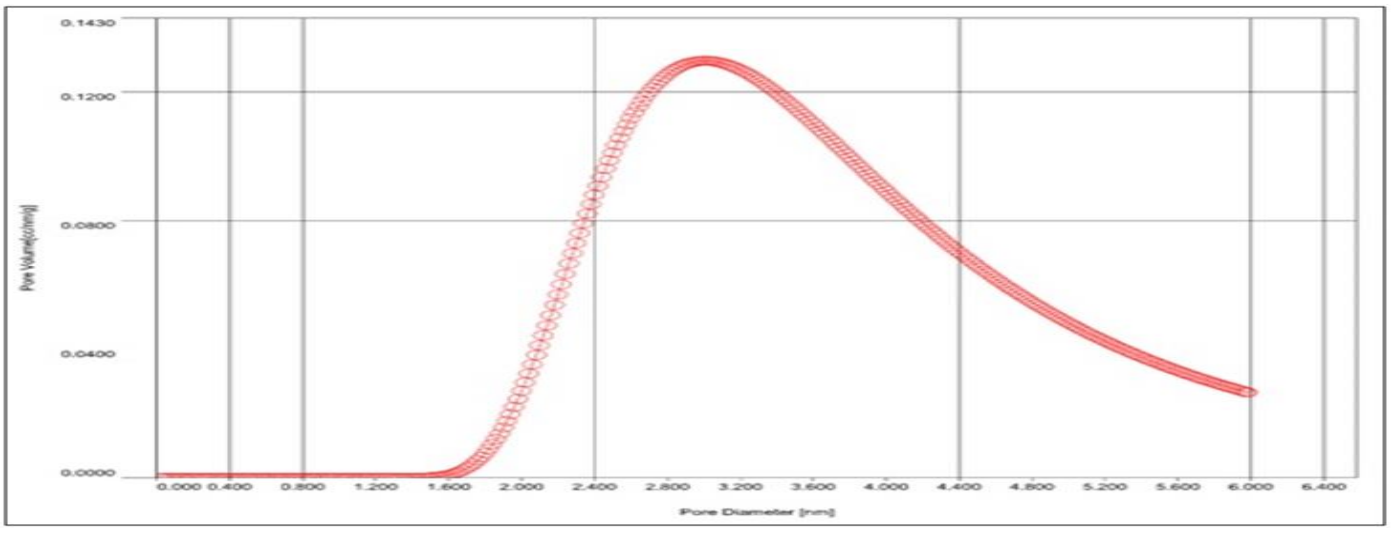

Fig 10 Dubinin-Astakhov (DA) Modal Pore Size Distribution for DDS Sample
Showing a Monolayer Adsorption Pore Diameter of 2.92nm

ISSN No:-2456-2165 https://doi.org/10.38124/ijisrt/IJISRT24JUN167

- *Ultimate/Elemental Analysis of Raw Materials of Doum Palm Shells (DPS), the African Elemi Shells (AES) and the Desert Date Shells (DDS):*

The elemental analysis of materials is regularly a critical parameter in product quality and safety and in Chemistry it is used to determine the elemental composition of chemical compounds and their composites. This is because raw materials analysis provides data for gaining insight into existing materials or helping to determine potential changes as a consequence of treatments. While the ultimate analysis is to evaluate the proportion of five major elements such as Carbon (C), Hydrogen (H), Nitrogen (N), Oxygen and Sulphur (S). Hence, according to Chen and co-workers (2019a) ultimate analysis is otherwise referred as elementary analysis. The outcome of this analysis will be helpful in proper mixing of waste to achieve a suitable C/N ratio and mass balance (for chemical or thermal processes).

In this paper, the elemental analysis provides useful information about the elemental composition of the biomass. The results for the chemical composition of raw materials of Doum palm shells (DPS), the African elemi shells (AES) and the desert date shells (DDS) are presented in Table 2.

Table 2 Ultimate/Elemental Analysis of Biomass

Sample	Carbon	Hydrogen	Nitrogen	Sulphur	Oxygen	Ash
DPS	81.70	0.23	15.15	0.11	2.64	25.00
AES	85.17	0.30	13.09	0.08	1.64	30.24
DDS	77.51	0.12	19.10	0.13	3.14	23.69

Note: DPS = Doum Palm Shell, AES = African Elemi, DDS = Desert Date Shell

The table 2 shows the key findings of high carbon and nitrogen contents: DPS (81.7% C, 15.15% N), AES (85.17% C, 13.09% N), and DDS (77.51% C, 19.10% N). High carbon content indicates suitability for activated carbon production, as it enhances adsorption and porosity during carbonization. Nitrogen content also influences pore development and surface chemistry (Foo et al., 2012; Gayathiri et al., 2022).

Ash content, crucial for processes like gasification and combustion, is 23.69% for DPS, 30.24% for AES, and 25% for DDS. Previous studies showed that char from gasified materials, with active minerals and large surface areas, exhibited significant catalytic activity in depolymerizing tar compounds Tsekos, et al., 2020).

Carbon: Nitrogen Ratio: The C:N ratio is a quick way to evaluate the balance between two elements present in the soil that are both essential for crop growth and microbial health. The C:N ratio in the organic matter of agricultural soils ideally averages about 10:1. This is considered an indication of a dynamic equilibrium condition that can and should be maintained. When organic material is added to the soil in root residue, manure, corn stalks, etc., the increased carbon triggers microbial growth. If the amount of N in the added material is inadequate to support the increased growth of microbes, the microbes will absorb N from the soil and immobilize it in their tissues. This will deprive growing plants of nitrogen they need for immediate growth. As carbon breaks down, larger microbe numbers decrease and N is now released again into the soil. The more stable 10:1 C:N ratio can now be established. Cover crops, especially legumes, have C:N ratios generally less than 25:1. As a general rule, these plants decompose relatively quickly because the amount of carbon contained is offset by adequate amounts of nitrogen and N is not immobilized. Low nitrogen, high carbon residues, such as wheat straw, have low nutritional quality for microbes and take longer to decompose. C:N ratios also provide clues about the microbial population present, as higher ratios tend to support more fungi present in the soil than bacteria.

The proportion of carbon to nitrogen in the organic matter is an important factor in controlling microbial activity. Organic material having a high carbon to nitrogen ratio (C/N), such as wheat straw at about 80/1, will decay relatively slowly because the material contains insufficient nitrogen to satisfy the growth requirements of the decay producing microorganisms. Soil microorganisms often retain the available nitrogen for prolonged periods. This nitrogen immobilization by microbes can create nitrogen deficiencies in the soil and lead to reduced plant growth. Legume residues, such as clovers and alfalfa, have low C/N ratios (< 30/1) and decay very rapidly in the soil. They release large amounts of CO_2 and some nutrients for plant growth. Materials from young plants, having low C/N ratios, decompose more rapidly than do materials from old plants, having higher C/N ratios. A list of common organic materials and their C/N ratios is provided in Table 3.

Table 3 Carbon: Nitrogen Ratio

Sample	Carbon	Nitrogen	C:N Ratio
DPS	81.70	15.15	5.39:1
AES	85.17	13.09	6.51:1
DDS	77.51	19.10	4.08:1

Note: DPS = Doum Palm Shell, AES = African Elemi, DDS = Desert Date Shell

SEM EDX Analysis of Raw materials of Doum palm shells (DPS), the African elemi shells (AES) and the desert date shells (DDS): The SEM EDX study (Fig. 11-13) reveals surface irregularities, heterogenic pore structures, fractured

ISSN No:-2456-2165 https://doi.org/10.38124/ijisrt/IJISRT24JUN167

cavities, and rough surfaces with slit cracks. DPS and DDS samples show significant pore growth and variously sized cavities. DDS has more craters and a more erratic, flaky surface compared to AES. BET data indicates mesoporosity in DPS and DDS due to these cavities. AES exhibits laminated surface microporosity, correlating to a high surface area, as seen in BET data.

FTIR results (Fig. 15) indicate functional groups like hydroxyl (-OH) in DPS and DDS, which are crucial for adsorption and may enhance adsorption capacity. EDX analysis confirms high carbon content in all samples, with AES having the highest atomic carbon proportion, making it an effective sorption material. High carbon content is preferred for superior activated carbon production (Aimikhe et al., 2022).

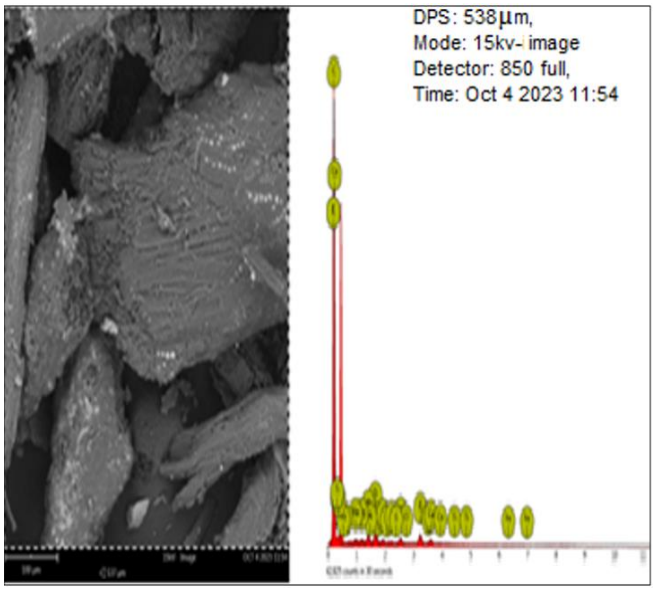

Fig 11 A SEM Micrographs and EDX Analysis of DPS Sample

Table 4 Elemental Composition of DPS Sample Obtained From SEM Micrographs and EDX Analysis

Element Number	Element Symbol	Element Name	Atomic Conc.	Weight Conc.
6	C	Carbon	81.70	76.39
7	N	Nitrogen	15.55	16.95
14	Si	Silicon	0.67	1.47
19	K	Potassium	0.42	1.29
13	Al	Aluminium	0.45	0.94
17	Cl	Chlorine	0.24	0.68
20	Ca	Calcium	0.19	0.58
11	Na	Sodium	0.27	0.48
15	P	Phosphorus	0.17	0.40
12	Mg	Magnesium	0.20	0.38
16	S	Sulfur	0.11	0.27
26	Fe	Iron	0.04	0.17
22	Ti	Titanium	0.00	0.00

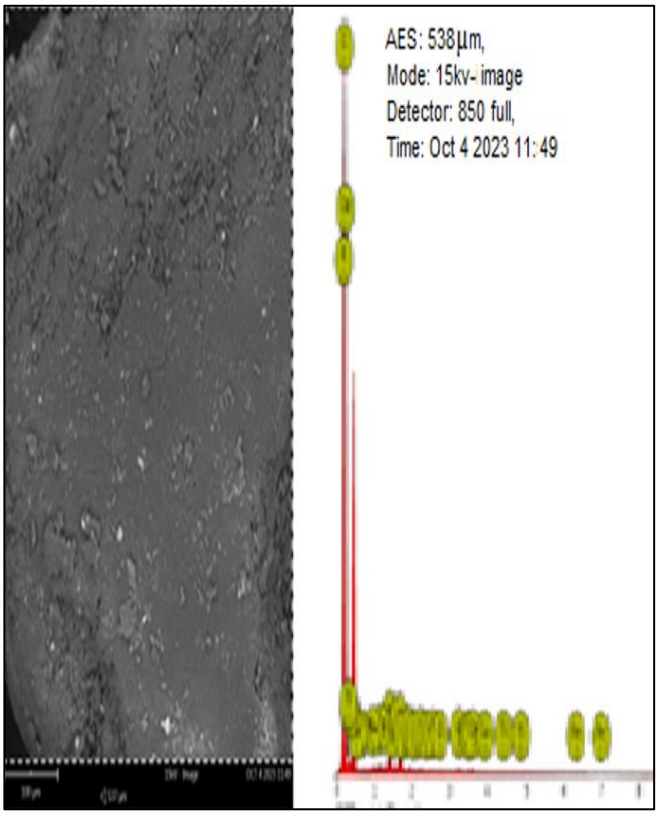

Fig 12 A SEM Micrographs and EDX Analysis of AES Sample

Table 5 Elemental Composition of AES Sample Obtained From SEM Micrographs and EDX Analysis

Element Number	Element Symbol	Element Name	Atomic Conc.	Weight Conc.
6	C	Carbon	85.17	81.67
7	N	Nitrogen	13.29	14.86
13	Al	Aluminium	0.46	0.99
14	Si	Silicon	0.34	0.77
12	Mg	Magnesium	0.19	0.37
11	Na	Sodium	0.18	0.33
15	P	Phosphorus	0.12	0.30
19	K	Potassium	0.07	0.22
16	S	Sulfur	0.08	0.22
20	Ca	Calcium	0.06	0.18
17	Cl	Chlorine	0.04	0.10
26	Fe	Iron	0.00	0.00
22	Ti	Titanium	0.00	0.00

ISSN No:-2456-2165 https://doi.org/10.38124/ijisrt/IJISRT24JUN167

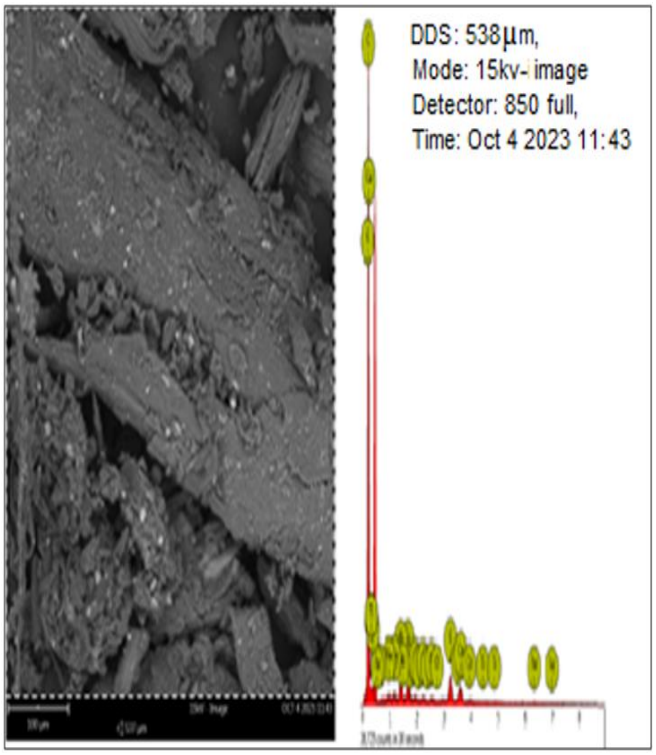

Fig. 13 A SEM Micrographs and EDX Analysis of DDS Sample

Table 6 Elemental Composition of DDS Sample Obtained From SEM Micrographs and EDX Analysis

Element Number	Element Symbol	Element Name	Atomic Conc.	Weight Conc.
6	C	Carbon	77.51	71.23
7	N	Nitrogen	19.22	20.59
19	K	Potassium	0.76	2.29
20	Ca	Calcium	0.44	1.36
13	Al	Aluminium	0.58	1.20
14	Si	Silicon	0.51	1.09
11	Na	Sodium	0.27	0.48
12	Mg	Magnesium	0.22	0.41
26	Fe	Iron	0.09	0.38
15	P	Phosphorus	0.15	0.35
16	S	Sulfur	0.13	0.33
17	Cl	Chlorine	0.11	0.30
22	Ti	Titanium	0.00	0.00

XRS-FP Analysis of Raw materials of Doum palm shells (DPS), the African elemi shells (AES) and the desert date shells (DDS):

Table 7 XRS-FP Analysis for DPS, AES and DDS Sample

SAMPLE	SiO_2 (%)	Fe_2O_3 (%)	P_2O_5 (%)	SO_3 (%)	CaO (%)	MgO (%)	K_2O (%)	Al_2O_3 (%)	TiO_2 (%)	Cl(%)
DPS	20.425	-	-	-	13.566	-	32.814	9.773	-	11.624
AES	34.995	5.334	1.367	2.858	7.572	17.581	8.148	11.979	1.168	6.503
DDS	14.279	6.367	1.109	2.863	25.696	-	34.132	6.764	-	4.047

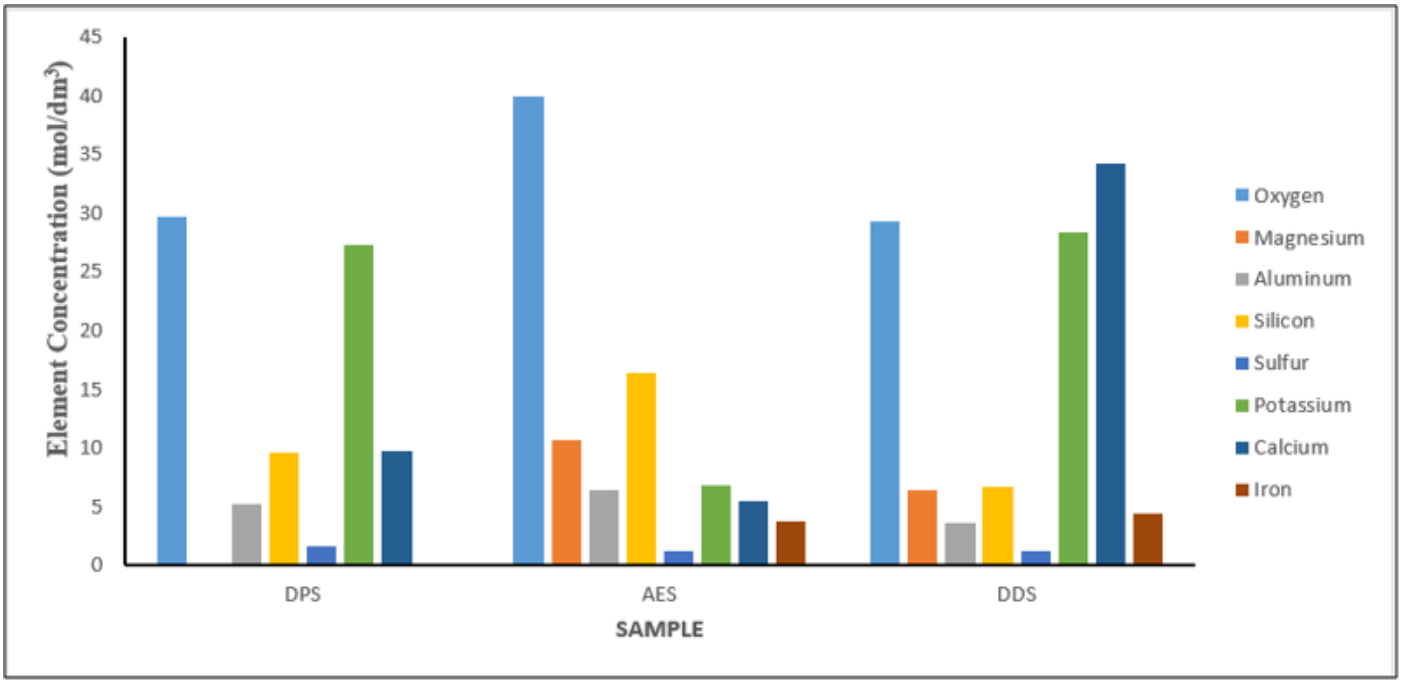

Fig 14 Element Concentrations of DPS, AES and DDS Sample Doum Palm Shells (DPS), the African Elemi Shells (AES) and the Desert Date Shells (DDS)

ISSN No:-2456-2165 https://doi.org/10.38124/ijisrt/IJISRT24JUN167

The XRF analysis reveals the elemental compositions of Doum palm shell (DPS), African elemi shell (AES), and Desert date shell (DDS), essential for evaluating their suitability for activated carbon synthesis.

Table 3 and Figure 14 show significant concentrations of SiO_2, CaO, Al_2O_3, K_2O, and Cl in DPS, AES, and DDS. For DPS, these are 20.425%, 13.566%, 32.814%, 9.773%, and 11.624% respectively. AES shows high levels of SiO2 (34.995%), MgO (17.581%), and Al2O3 (11.979%), while DDS contains SiO2 (14.279%), CaO (25.696%), and K2O (34.132%).

High concentrations of these elements may increase ash content in activated carbon, affecting its porosity and adsorption properties. Optimizing precursors and possibly applying customized pre-treatments or activation methods can minimize ash content and enhance adsorption properties in AES and DDS due to their higher CaO, MgO, and K_2O levels (Boruah et al., 2021; Chen and Bie, 2020; Chowdhury et al., 2016 and Daood et al 2014).

Fourier transform infrared (FTIR) spectra Analysis of Raw materials of Doum palm shells (DPS), the African elemi shells (AES) and the desert date shells (DDS): The FTIR method is crucial for locating and identifying distinctive functional groups in any given material. Figure 3.8 displays the results of the AES and DPS samples' FTIR analysis. The DPS and AES results show comparable patterns, with their peaks located approximately at 3084.15 cm^{-1}, 1979.50 cm^{-1}, 1577.88 cm^{-1}, and 1058.30 cm^{-1}, respectively, signifying the presence of hydrocarbons or aromatic C–H stretching, aromatic C=C stretching, phenolic C=C stretching, and hydroxyl groups C–O stretching. In contrast to DPS and AES, the DDS sample has several peaks. O-H stretching vibrations of hydroxyl groups (alcohols and phenols) were linked to the FTIR result for the DDS sample, which showed peaks at around 3629.47 cm^{-1}, 3532.77 cm^{-1}, and 3390.18 cm^{-1}. Peaks located at around 3056.72 cm^{-1}, 3025.02 cm^{-1}, 2922.03 cm^{-1}, and 2849.41 cm^{-1} may be indicative of the presence of organic molecules due to C-H stretching vibrations in alkanes and alkyl groups. Peak at 2183.94 cm^{-1} suggests the existence of C≡C triple bonds, which may be a sign of nitriles or alkynes. The peak range of 2050.49 - 1451.31) cm^{-1} is linked to several functional groups found in aromatic compounds, such as aromatic rings (C=C stretching vibrations), carbonyl groups (C=O stretching vibrations), and bending vibrations in C-H.

According to Aimikhe *et al.,* 2022 the presence of functional groups such as hydroxyl (-OH), carbonyl (C=O), and aromatic structures on the activated carbon surface indicates possible active sites. By offering locations for chemical interactions, these functional groups may improve sorption capacities and influence its adsorption characteristics, selectivity, and affinity for certain pollutants.

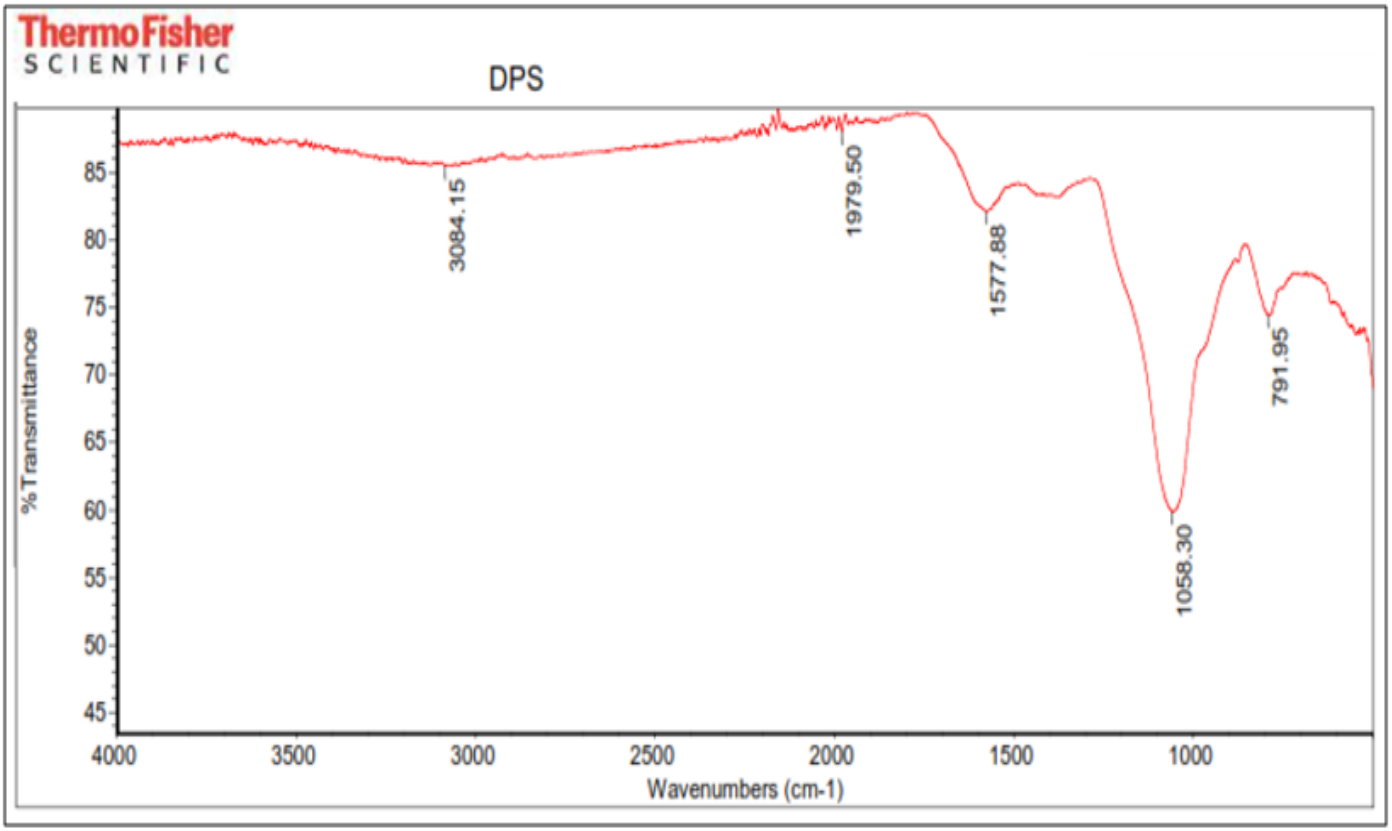

Fig 15 A Fourier Transform Infrared (FTIR) Spectroscopic Analysis of DPS Samples

ISSN No:-2456-2165 https://doi.org/10.38124/ijisrt/IJISRT24JUN167

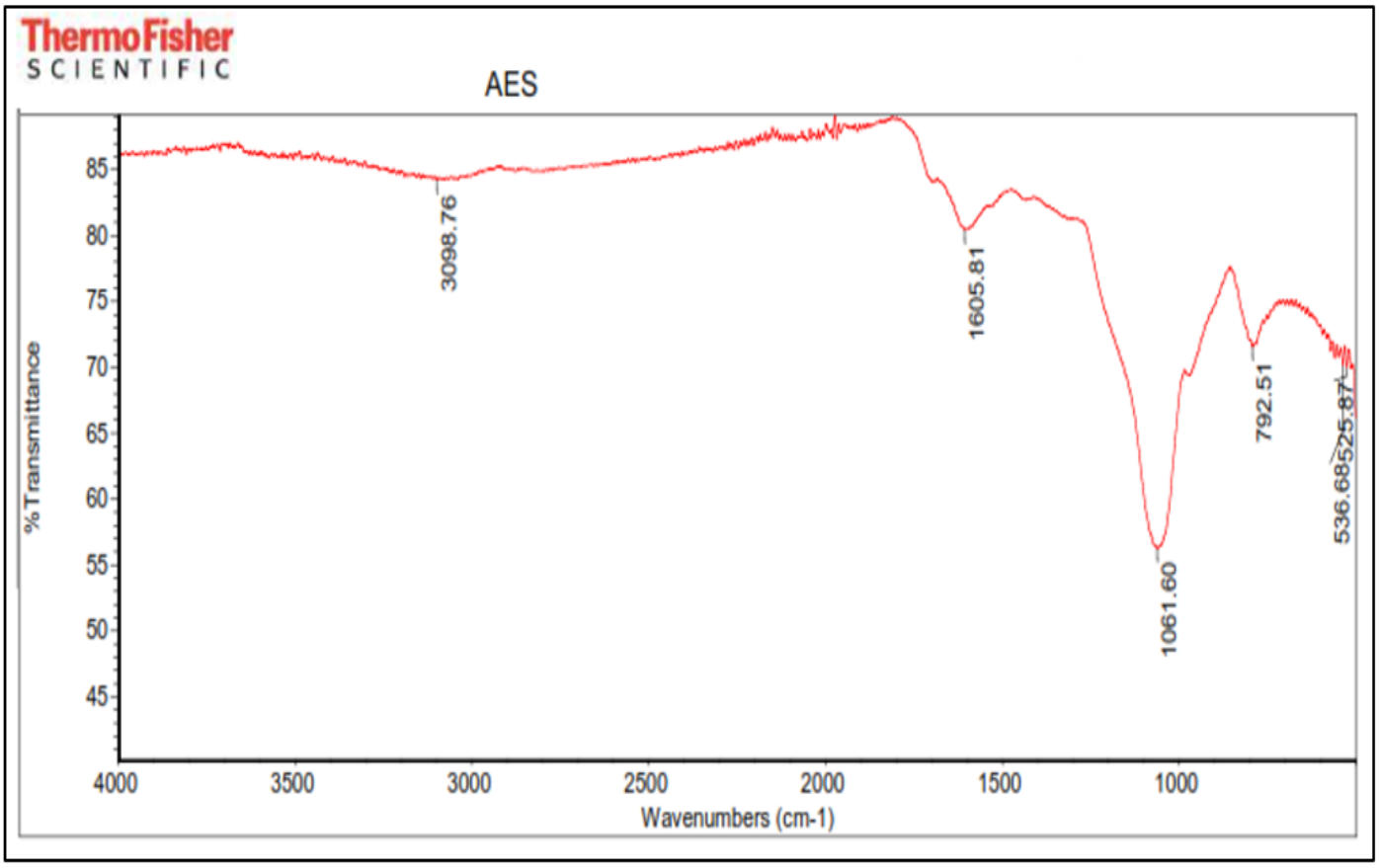

Fig 16 b Fourier Transform Infrared (FTIR) Spectroscopic Analysis of AES Samples

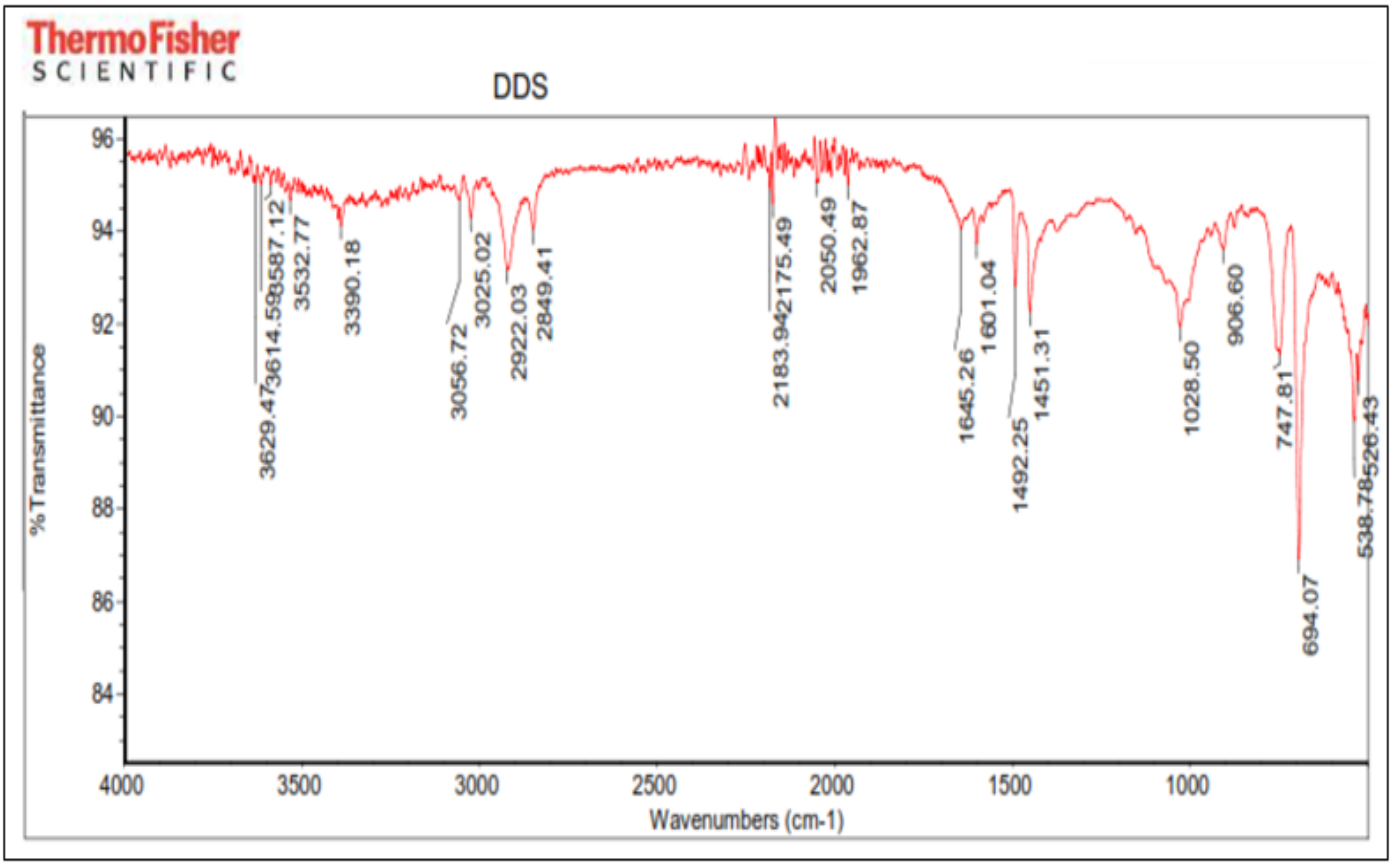

Fig 17 c Fourier Transform Infrared (FTIR) Spectroscopic Analysis of DDS Samples

ISSN No:-2456-2165 https://doi.org/10.38124/ijisrt/IJISRT24JUN167

Table 8 Comparison of BET Surface Area of this Study and Selected Published Literature.

SAMPLES	BET(m^2/g)	References
DPS	285.00	This study
AES	471.00	This study
DDS	418.00	This study
Corn cob	1.80	[28]
Rice straw	4.90	[28]
Water hyacinth	4.70	[28]
Rice husk	230.91	[11]
Empty fruit bunch	15.42	[11]
Rice Husk	250.00	[11]
Rice husk	178.00	[24]
Egg shells	273.00	[18]
Peanut shells	1.83	[5]
Almond shells	11.27	[5]
Groundnut shells	32.96	[6]
Avocado seed	1.75	[23]
Pinecone	0.25	[12]
Raw pomegranate peel	598.78	[7]
Sugarcane bagasse pith	500.00	[21]
Jack fruit leaf powder	246.90	[9]
Guava leaves	100.76	[1]
Olive stone	400.00	[34]
Coconut shells	437.00	[24]

IV. CONCLUSION:

The research findings highlight Doum palm shells (DPS), African elemi shells (AES), and desert date shells (DDS) as promising materials for adsorption. These shells showed high volatile matter, low ash, and high carbon content, making them efficient adsorbents. Specific surface area, pore volume, and pore size analyses confirmed their microporous nature, enhancing their adsorption potential. Elemental composition, particularly SiO2, CaO, Al2O3, K2O, and Cl, suggests the need for tailored activation processes, as shown by XRF analysis. SEM and FTIR studies revealed surface morphology and functional groups, indicating potential adsorption sites. Overall, this comprehensive characterization supports further investigation and application in adsorption processes, emphasizing the need for customization based on elemental composition and surface properties. Thus, results revealed that the high carbon atomic concentration of the AES DPS and DDS sample makes them suitable materials for modification for adsorption application. Doum palm shells (DPS), African elemi shells (AES), and desert date shells (DDS) is Type I microporous solids with a BJH pore diameter of 2.14, 2.13 and 2.10 nm respectively and BET surface areas of 285, 471 and 418 m^2 /g, and DFT surface area of 77, 114, 87 m^2 /g respectively. The DPS, AES, and DDS sample, which exhibits potential efficacy as an adsorbent, may be used or subjected to further modifications for adsorption applications.

Conflicts of Interest: The authors declare no conflicts of interest.

REFERENCES

[1]. Abdelfattah, I., Ismail, A. A., Al Sayed, F., Almedolab, A., & Aboelghait, K. M. (2016). Biosorption of heavy metals ions in real industrial wastewater using peanut husk as efficient and cost-effective adsorbent. Environmental Nanotechnology, Monitoring & Management, 6, 176-183.

[2]. Adowei, P. (2024). Fixed-Bed Column Adsorption Studies of Synthetic Organic Chemicals Using Carbonized and Surface-Modified Carbons from Nipa Palm Leaves. International Journal of Environmental Chemistry, 8(1), 1-11. https://doi.org/10.11648/j.ijec.20240801.11

[3]. Aimikhe, V. J., Anyebe, M. S., & Ibezim-Ezeani, M. (2022). Development of composite activated carbon from mango and almond seed shells for CO2 capture. *Biomass Conversion and Biorefinery*, 1-15.

[4]. Akande OM, Olorunnisola AO. Potential of briquetting as a waste-management option for handling market-generated vegetable waste in Port Harcourt, Nigeria. Recycling. 2018;3(2):11. DOI: 10.3390/recycling3020011

[5]. ASTM D3176-09, ASTM International (2009) Standard practice for ultimate analysis of coal and coke. ASTM International, Pennsylvania. doi:10.1520/D3176-09

[6]. ASTM D5373-08 (2008) Standard test methods for instrumental determination of carbon, hydrogen, and nitrogen in laboratory samples of coal. doi: 10.1520/D5373-08

ISSN No:-2456-2165 https://doi.org/10.38124/ijisrt/IJISRT24JUN167

[7]. Bilal, H., Li, X., Iqbal, M. S., Mu, Y., Tulcan, R. X. S., & Ghufran, M. A. (2023). Surface water quality, public health, and ecological risks in Bangladesh—a systematic review and meta-analysis over the last two decades. *Environmental Science and Pollution Research*, *30*(40), 91710-91728.

[8]. Buddy D. Ratner (2013). Surface Properties and Surface Characterization of Biomaterials. In book: Biomaterials Science DOI: 10.1016/B978-0-08-087780-8.00005-X

[9]. Chen, P., & Bie, R. (2020). Nano-Silica Production by Rice Husk Combustion in a 0.7 MW Double-Circulating Fluidized Bed after Acid Pretreatment [J]. Journal of Harbin Institute of Technology (New Series), 27(4), 8-19.

[10]. Chowdhury, Z. Z., Karim, M. Z., Ashraf, M. A., & Khalid, K. (2016). Influence of carbonization temperature on physicochemical properties of biochar derived from slow pyrolysis of durian wood (Durio zibethinus) sawdust. BioResources, 11(2), 3356-3372.

[11]. Dawood, S., Sen, T. K., & Phan, C. (2014). Synthesis and characterisation of novel-activated carbon from waste biomass pine cone and its application in the removal of congo red dye from aqueous solution by adsorption. Water, Air, & Soil Pollution, 225, 1-16.

[12]. Erans, M., Sanz-Pérez, E. S., Hanak, D. P., Clulow, Z., Reiner, D. M., & Mutch, G. A. (2022). Direct air capture: process technology, techno-economic and socio-political challenges. *Energy & Environmental Science*, *15*(4), 1360-1405.

[13]. Foo, K. Y., & Hameed, B. H. (2012). Textural porosity, surface chemistry and adsorptive properties of durian shell derived activated carbon prepared by microwave assisted NaOH activation. *Chemical engineering journal*, *187*, 53-62.

[14]. Gayathiri, M., Pulingam, T., Lee, K. T., & Sudesh, K. (2022). Activated carbon from biomass waste precursors: Factors affecting production and adsorption mechanism. *Chemosphere*, *294*, 133764.

[15]. Grennfelt, P., Engleryd, A., Forsius, M., Hov, Ø., Rodhe, H., & Cowling, E. (2020). Acid rain and air pollution: 50 years of progress in environmental science and policy. *Ambio*, *49*, 849-864.

[16]. Ikram, M., Rehman, A. U., Ali, S., Ali, S., Bakhtiar, S. U. H., & Alam, S. (2016). The adsorptive potential of chicken egg shells for the removal of oxalic acid from wastewater. Journal of Environmental Sciences, 2(2), 118-131

[17]. Kainth, S., Sharma, P., & Pandey, O. P. (2024). Green sorbents from agricultural wastes: A review of sustainable adsorption materials. *Applied Surface Science Advances*, *19*, 100562.

[18]. Kumar, A., & Jena, H. M. (2015). High surface area microporous activated carbons prepared from Fox nut (Euryale ferox) shell by zinc chloride activation. *Applied Surface Science*, *356*, 753-761.

[19]. Merrett K, Cornelius RM, McClung WG, Unsworth LD, Sheardown H. Surface analysis methods for characterizing polymeric biomaterials. J Biomater Sci Polym Ed. 2002;13(6):593-621. doi: 10.1163/156856202320269111. PMID: 12182547.

[20]. Sangeetha A., Rabitha R., Sivasree B., Nivedha B., Stanlin J.S., Arun C., Shanmugam K. and Balakumar P. (2023), Adsorbent potential of the leaf powder of artocarpus heterophyllus lam (jackfruit) in efficiently removing hexavalent chromium from landfill leachate, Global NEST Journal, 25(9), 88-96.

[21]. Shoaib, A. G., El-Sikaily, A., El Nemr, A., Mohamed, A. E. D. A., & Hassan, A. A. (2020). Preparation and characterization of highly surface area activated carbons followed type IV from marine red alga (Pterocladia capillacea) by zinc chloride activation. *Biomass Conversion and Biorefinery*, 1-13.

[22]. Tsekos, C., Anastasakis, K., Schoenmakers, P. L., & de Jong, W. (2020). PAH sampling and quantification from woody biomass fast pyrolysis in a pyroprobe reactor with a modified tar sampling system. *Journal of Analytical and Applied Pyrolysis*, *147*, 104802

[23]. Wahby, A., Abdelouahab-Reddam, Z., El Mail, R., Stitou, M., Silvestre-Albero, J., Sepúlveda-Escribano, A., & Rodríguez-Reinoso, F. (2011). Mercury removal from aqueous solution by adsorption on activated carbons prepared from olive stones. Adsorption, 17, 603-609.

[24]. Wang, H and Chu, Paul K (2013). Characterization of Biomaterials. Pages 105-174. Chapter 4 – Surface https://doi.org/10.1016/B978-0-12-415800-9.00004-8

[25]. Wang SR, Ru B, Dai GX, Sun WX, Qiu KZ, Zhou JS. Pyrolysis mechanism study of minimally damaged hemicellulose polymers isolated from agricultural waste straw samples. Bioresource Technology. 2015;190:211-218

[26]. Yangyang L, Jin Y, Li J, Chen Y, Gong Y, Li Y, et al. Current situation and development of kitchen waste treatment in China. In: The Tenth International Conference on Waste Management and Technology (ICWMT), Procedia Environmental Sciences. Vol. 31. 2016. pp. 40-49

[27]. Zak, D., Hupfer, M., Cabezas, A., Jurasinski, G., Audet, J., Kleeberg, A., McInnes, R., Kristiansen, S.M., Petersen, R.J., Liu, H & Goldhammer, T. (2021). Sulphate in freshwater ecosystems: A review of sources, biogeochemical cycles, ecotoxicological effects and bioremediation. *Earth-Science Reviews*, *212*, 103446.